Author Manuscript

Author Manuscript

Author Manuscript

Author Manuscript

HHS Public Access

Author manuscript

Clin Cancer Res. Author manuscript; available in PMC 2020 May 01.

Published in final edited form as:

Clin Cancer Res. 2019 November 01; 25(21): 6501–6510. doi:10.1158/1078-0432.CCR-19-0289.

Characterization and comparison of GITR expression in solid tumors

Luis M Vence[1,*], **Samantha L Bucktrout**[2,3,*], **Irina Fernandez**[1], **Jorge M Blando**[1], **Bevin M Smith**[2], **Ashley E Mahne**[2], **John C Lin**[2,4], **Terrence Park**[2], **Edward Pascua**[2], **Tao Sai**[2], **Javier Chaparro-Riggers**[2], **Sumit K Subudhi**[5], **Jorge A Scutti**[1], **Maria G Higa**[1], **Hao Zhao**[1], **Shalini S Yadav**[1], **Anirban Maitra**[6], **Ignacio I Wistuba**[7], **James P Allison**[1,8], **Padmanee Sharma**[1,5]

[1]The Immunotherapy Platform, The University of Texas MD Anderson Cancer Center, Houston, TX 77054, USA

[2]Cancer Immunology Discovery Unit, Pfizer Inc., 230 E. Grand Ave, South San-Francisco, CA 94080, USA

[3]Parker Institute for Cancer Immunotherapy, 1 Letterman Drive, Suite D-3500, San Francisco, CA 94129, USA

[4]Regeneron Pharmaceuticals Inc., Tarrytown, NY 10591, USA

[5]Department of Genitourinary Medical Oncology, The University of Texas MD Anderson Cancer Center, Houston, TX 77030, USA

[6]Department of Pathology, The University of Texas MD Anderson Cancer Center, Houston, TX 77030, USA

[7]Department of Translational Molecular Pathology, The University of Texas MD Anderson Cancer Center, Houston, TX 77030, USA

[8]Department of Immunology, The University of Texas MD Anderson Cancer Center, Houston, TX 77030, USA

Abstract

Corresponding author: Padmanee Sharma, M.D., Ph.D., Genitourinary Medical Oncology, Unit 1374, 1155 Pressler St., Houston TX 77030, Tel: 713-792-2830, Fax: 713-745-0422, padsharma@mdanderson.org.

*These authors contributed equally to the manuscript.

Conflict-of-interest disclosure:

JP Allison is an inventor and recipient of royalties from intellectual property licensed to Bristol-Meyer Squibb, Merck, and Jounce. He is a member of the scientific advisory board for Jounce Therapeutics, Neon Therapeutics, Amgen, Apricity, BioAtla, Forty-Seven, Polaris, Tvardi Therapeutics, Hummingbird, Merck & Co., BMS and Dragonfly therapeutics, ImaginAB, Codiak Biosciences, and Marker Therapeutics. He has stock ownership in Jounce Therapeutics, Neon Therapeutics. BioAtla, Forty-Seven, Apricity, Polaris, Marker Therapeutics, Codiak Biosciences, ImaginAB, Hummingbird, Optera, Tvardi therapeutics, and Dragonfly Therapeutics. JP Allison and P Sharma own a patent licensed to Jounce Therapeutics. P Sharma serves as a consultant for Constellation, Jounce Therapeutics, Neon Therapeutics, BioAtla, Pieris Pharmaceuticals, Oncolytics Biotech, Merck, BioMx, Forty-Seven, Polaris, Apricity, Marker Therapeutics, Codiak, ImaginAB, Hummingbird, Optera and Dragonfly. She also has stock ownership in Jounce, Neon Therapeutics, Constellation, Oncolytics, BioAtla, Forty-Seven, Apricity, Polaris, Marker Therapeutics, Codiak, ImaginAB, Hummingbird, Optera, and Dragonfly. All other authors have no conflicts of interest to disclose.

Author Manuscript Author Manuscript Author Manuscript Author Manuscript

Purpose: Determine the differential effect of a FcγR-binding, mIgG2a anti-GITR antibody in mouse tumor models and characterize the tumor microenvironment for the frequency of GITR expression in T cell subsets from seven different human solid tumors.

Experimental Design: For mouse experiments, wildtype C57BL/6 mice were subcutaneously injected with MC38 cells or B16 cells, and BALB/c mice were injected with CT26 cells. Mice were treated with the anti-mouse GITR agonist antibody 21B6, and tumor burden and survival were monitored. GITR expression was evaluated at the single cell level using flow cytometry (FC). 213 samples were evaluated for GITR expression by immunohistochemistry (IHC), 63 by FC and 170 by both in seven human solid tumors: advanced hepatocellular carcinoma, non-small cell lung cancer, renal cell carcinoma, pancreatic carcinoma, head and neck carcinoma, melanoma, and ovarian carcinoma.

Results: The therapeutic benefit of 21B6 was greatest in CT26 followed by MC38, and was least in the B16 tumor model. The frequency of CD8 T cells and effector CD4 T cells within the immune infiltrate correlated with response to treatment with GITR antibody. Analysis of clinical tumor samples showed that non-small cell lung cancer, renal cell carcinoma, and melanoma had the highest proportions of GITR-expressing cells and highest per-cell density of GITR expression on CD4-positive Foxp3 positive Tregs. IHC and FC data showed similar trends with a good correlation between both techniques.

Conclusions: Human tumor data suggest that NSCLC, RCC, and melanoma should be the tumor subtypes prioritized for anti-GITR therapy development.

Keywords

GITR; solid tumors; cancer; immunotherapy; Immunohistochemistry

INTRODUCTION

Cancer therapies targeting immune checkpoints that are members of the CD28/B7 superfamily (e.g., CTLA-4, PD-1, and PD-L1) have demonstrated a survival benefit in several malignancies, including melanoma (1–4), renal cell carcinoma (5), non-small cell lung cancer (6,7), urothelial carcinoma (8), and Hodgkin's lymphoma (9). Despite their success as monotherapies, these immune checkpoint blockers fail to induce responses in the majority of patients. Although response rates can be improved by simultaneously targeting PD-1 (with nivolumab) and CTLA-4 (with ipilimumab), this combination also induces a significantly higher rate of treatment-related grade 3-4 toxicities (10). Interestingly, a subgroup analysis demonstrated that progression-free survival was similar for patients with PD-L1-positive melanoma treated with the combination versus nivolumab alone (10). This finding suggests that it would be beneficial to establish predictive biomarkers to identify patients in whom nivolumab alone is sufficient or patients in whom other checkpoint combinations may maximize therapeutic success while minimizing toxicities. For example, nonsynonymous mutation and neoantigen load, the presence and location of CD8 T cells, and expression of the receptor or ligand have all been shown to identify patients most likely to respond to therapies targeting the PD-1/PDL1 pathway (11–14). With the exception of CD8 T cells, other markers have inconsistencies and their predictive value depends on the

Author Manuscript Author Manuscript Author Manuscript Author Manuscript

tumor type. Other immune checkpoints currently being evaluated in the clinic as potential targets include members of the TNF family, such as 4-1BB, OX40, and glucocorticoid-induced TNFR-related protein (GITR).

GITR is a cell-surface protein that is expressed at high levels on activated CD4 and CD8 T cells (15–17) and FoxP3-positive ($FoxP3^+$) T regulatory cells (Tregs) (18), at intermediate levels on natural killer (NK) cells (19), and at low levels on naïve T cells, macrophages, and B cells (18,20). Signaling through GITR enhances T cell proliferation and effector functions (21,22) and protects T cells from activation-induced cell death, which in turn increases the frequency of memory T cells. In preclinical studies, the anti-mouse GITR monoclonal antibody DTA-1, which is a rat IgG2a antibody, demonstrated anti-tumor activity (23–25). DTA-1 demonstrated additive anti-tumor activity in combination with anti-CTLA-4 (26) and anti-PD-1 (27). A humanized IgG1 non-Fc receptor binding mutant agonist anti-human GITR monoclonal antibody (TRX518) is currently being evaluated in two clinical trials: a dose-escalation phase I trial in patients with advanced refractory solid tumors () and a Phase I trial in patients with stage III or IV malignant melanoma or other solid tumors (TRX518-001). In the dose-escalation trial (), a single dose of TRX518 of up to 8 mg/kg was well tolerated with no dose-limiting toxicities or serious treatment-related adverse events (28). This single dose was sufficient to reduce Treg levels both in the circulation and the tumor of treated patients. Interestingly, the level of GITR expression measured at baseline correlated with the decrease in Tregs. This is likely due to the subpopulation of Tregs preferentially affected was the antigen-experienced effector Tregs ($CD45RA^-$ $Foxp3^{high}$), which express higher levels of GITR than naïve Tregs do. The proposed mechanism for this effect is destabilization of the Treg phenotype following agonist antibody binding, resulting in down-regulation of Foxp3 and increased expression of T-bet (the main Th1-lineage transcription factor), and not an effect on the proliferative capacity of Tregs (29). Other GITR antibodies currently being evaluated in clinical trials are of hIgG1 isotype, which has a bias for activating Fcγ**R** binding and is thus highly likely to induce antibody-dependent cell cytotoxicity or antibody-dependent cell phagocytosis (30). The proposed mechanism of action of hIgG1 GITR monoclonal antibody is binding $GITR^{high}$ cells and, via Fc antibody-dependent cell cytotoxicity or cell phagocytosis, resulting in cell depletion (31). In mice treated with DTA-1, tumor-infiltrating Tregs are preferentially depleted over peripheral Tregs and tumor $CD8^+$ T cells, resulting in tumor growth inhibition. This selective depletion is likely due to higher GITR expression on tumor-infiltrating Tregs than peripheral Tregs or other immune cells infiltrating the solid tumor (30,32).

In this study, we characterized the differential anti-tumor effect of a mIgG2a anti-GITR antibody in mouse tumor models and evaluated the relationship between anti-tumor effect and the pattern and level of GITR expression in the tumor microenvironment. To examine potential translatability of mouse results to human, we also characterized the tumor microenvironment for the pattern and level of GITR expression in T cell subsets from seven different human solid tumors using immunohistochemistry (IHC) and/or flow cytometry (FC). The data presented here give insights into which solid tumors should be prioritized for the clinical development of anti-GITR therapies.

Author Manuscript Author Manuscript Author Manuscript Author Manuscript

MATERIALS AND METHODS

Mice and reagents.

Wildtype C57BL/6 and BALB/c mice were obtained from The Jackson Laboratories (Bar Harbor, ME) and housed in a pathogen-free facility at Pfizer (South San Francisco, CA) in accordance with the Institutional Animal Care and Use Committee protocol R.340 at Pfizer.

The CT26 (CRL-2638) mouse colon carcinoma cell line and the B16-F10 (CRL-6475) mouse melanoma cell line were obtained from the American Type Culture Collection (Manassas, VA). The MC38 mouse colon carcinoma cell line was a gift from Dr. Antoni Ribas at University of California, Los Angeles, (2011). Tumor cell lines were propagated in DMEM with 4.5 g/L glucose, L-glutamine, and sodium pyruvate (10-013-CV, Mediatech, Inc., Manassas, VA) containing 10% FBS and 1% penicillin–streptomycin solution (Thermo Fisher Scientific, Waltham, MA). All frozen stocks were cultured and passaged twice before implantation.

Anti-mGITR 21B6 heavy and light chain variable domain DNA sequences were obtained from cDNA generated using RT-PCR from a Lewis rat hybridoma fusion. The resulting translated amino acid sequence was codon-optimized for human epithelial kidney 293 expression using proprietary algorithms from Thermo Fisher Scientific Geneart. Synthesized codon-optimized variable domains were then cloned into the mammalian expression vectors pARC mIgG2a and pARC mKappa using *Bss*HII/*Bst*EII and *Apa*LI/*Pac*I, respectively. Correct clones for light and heavy chain constructs were sequence-confirmed.

Tumor challenge and treatment.

For syngeneic tumor experiments, 8- to 10-week old female mice were subcutaneously injected with 2×10^5 CT26 cells (Balb/c), 10^6 MC38 cells, or 5×10^5 B16 cells (C57BL/6). Tumor diameter was measured by digital calipers, and tumor volume was calculated by the formula $\frac{1}{2} L \times W^2$, where L (length) is defined as the longest diameter of the tumor and W (width) is perpendicular to L. Treatments were initiated when tumors reached an average volume of 85 mm^3. Mice were randomized into groups of 15 mice having nearly equal average tumor volumes and SEM. Either 21B6 antibody or an isotype control (C1.18.4, BioXcell, West Lebanon, NH) was dosed intraperitoneally at 1 mg/kg. Treatment began on the day of randomization and continued every 2 to 3 days for a total of three doses.

Tumor growth inhibition was calculated using the following formula: % tumor growth inhibition = $(1-T/T_0 / C/C_0) / (1-C_0/C) *100$, where C_0 = median pretreatment tumor volume of the control group, C = median final tumor volume of the control group, T_0 = median pretreatment tumor volume of the treatment group, and T = median final tumor volume of the treatment group. Complete tumor regression was assigned when tumors regressed and remained below the reliably measurable volume of 50 mm^3.

FC analysis of murine tumors.

Dissected tumors were dissociated using the Miltenyi Octet system (Miltenyi Biotec, San Diego, CA). Cells were washed with PBS and prepared for FACS analysis by labeling with

Author Manuscript Author Manuscript Author Manuscript Author Manuscript

LIVE/DEAD Fixable Violet stain (Thermo Fisher Scientific), anti-CD90.2 FITC (30-H12), anti-CD4 PE (GK1.5), and anti-CD8 BV786 (53-6.7), all from BD Biosciences (San Diego, CA, USA) and anti-GITR APC (DTA-1) and anti-CD45 PerCP/Cy5.5 (30-F11) and Foxp3 (FJK-16s) from eBioscience (San Diego, CA) following manufacturer's instructions.

FC analysis of human tumors.

Fresh tumor tissue was dissociated with a GentleMACS system (Miltenyi Biotec; Bergisch Gladbach, Germany) per the manufacturer's instructions and cultured overnight in a 96 well-plate with RPMI 1640 medium supplemented with 10% human AB Serum, 10 mM HEPES, 50 μM β-ME, penicillin/streptomycin/l-glutamine, and 50 U/ml human IL-2. The cells were subsequently harvested and stained with the following fluorescently conjugated monoclonal antibodies: anti-CD8 Alexa Fluor 700 (RPA-T8) and anti-CD127 BV711 (HIL-7R-M21), from BD Biosciences; anti-CD3 PerCP-Cy5.5 (UCHT1), from Biolegend (San Diego, CA, USA); anti-CD4 Alexa Fluor 532 (SK3), GITR-Alexa Fluor 488 (eBioAITR), and anti-FoxP3 PE-e610 (PCH101), from eBioscience; and Live/Dead fixable yellow stain, from Thermo Fisher (NY). Samples were acquired on a BD LSR Fortessa cytometer (BD Biosciences). FC data were analyzed using FlowJo software. After appropriate forward/side scatter and live cell gating, three peripheral T cell populations were identified: total effector CD8 T cells ($CD3^+CD8^+$), CD4 T cells ($CD3^+CD4^+FoxP3^{neg}$, Teff), and CD4 Tregs ($CD3^+CD4^+FoxP3^+CD127^{neg/low}$, Treg). GITR expression was assessed for each cell population and calculated as a percentage of total live cells. The gating strategy used is shown in Supplementary Figure 7.

IHC and hematoxylin-eosin staining were performed on tumor tissues that were fixed in 10% formalin, embedded in paraffin, and transversely sectioned (4 μm) on glass slides. For IHC tissues were stained with mouse anti-human monoclonal antibodies against CD3 (Dako, Cat #A0452), CD4 (Novocastra, CD4-368-L-A), CD8 (Thermo Fisher Scientific, MS-457-S), FoxP3 (BioLegend, Cat #320102), and GITR (Pfizer proprietary 10H2 [Lot XY110414], mouse IgG1, 1.07 mg/m). The slides were scanned and digitalized using a Scanscope XT system (Aperio/Leica Technologies) at 20X magnification. Quantitative analysis for each IHC marker was conducted by pathologists (who were blinded for clinic-pathological information) using ImageScope image analysis software (Aperio/Leica) and interpreted in conjunction with hematoxylin-eosin-stained sections. Five random areas (1 mm^2 each) were selected on each digital slide and a customized algorithm was used in order to determine the number of positive cells. The data are expressed as a percentage (total number of positive cells / total number of cells per area). Representative single stain images are shown in Supplementary Figures 8a–e.

Statistics.

For analysis of tumor growth curves, tumor volume data were log 10 transformed, and analysis of covariance (ANCOVA) was applied to the log-transformed data at each time point. Comparison of the treatment group to negative control at the final time point was performed in a 1-sided test. Survival data were analyzed using GraphPad Prism, version 7. Survival curves were compared by log-rank Mantel-Cox test.

Author Manuscript Author Manuscript Author Manuscript Author Manuscript

For IHC, ANOVA was used to compare percentages of cells expressing GITR, CD8, and CD4. Data were represented in a heat map using Qlucore software (Lund, Sweden). Data were log2 transformed for this representation. ANOVA followed by Tukey's multiple comparison test was used to compare percentages and MFI between different tumors and T cell subpopulations. R and R^2 were calculated using Excel (Microsoft, CA). In all graphs, * represents, $p \leq 0.05$; **, $p \leq 0.01$; ***, $p \leq 0.001$; ****, $p \leq 0.0001$. For correlation analysis between IHC and FC, the median value for GITR, CD3, CD4, CD8, and FoxP3 expression obtained by IHC was plotted against the median value of the same marker measured by FC for the three tumor types (HCC, NSCLC, and RCC).

RESULTS

The anti-tumor efficacy of a GITR antibody varies across mouse tumor models.

The GITR agonistic antibody DTA-1 with a mIgG2a Fc has been reported to cause complete tumor growth inhibition and enhanced survival in the syngeneic murine colon adenocarcinoma model CT26 (33). We tested another anti-murine GITR antibody, 21B6, with a mouse IgG2a Fc, and demonstrated anti-tumor activity similar to that of DTA-1. 21B6 caused 94% growth inhibition of CT26 tumors and enhanced survival (Figure 1a–d). In another syngeneic murine colon adenocarcinoma model, MC38, the same therapeutic regimen with 21B6 caused 58% tumor growth inhibition (Figure 1e–g); the effect on survival could not be determined in this model due to tumor ulceration. In the B16 melanoma model, 21B6 caused 28% tumor growth inhibition with little survival benefit (Figure 1h–k). Together, these data show that an anti-mouse GITR antibody has the greatest therapeutic benefit in the CT26 tumor model, less benefit in the MC38 tumor model, and least benefit in the B16 tumor model.

The frequency of effector CD8 and CD4 T cells correlates with response to anti-GITR antibody in mouse tumor models.

We next asked if any immune biomarkers correlated with the ranked efficacy of the GITR antibody in the CT26, MC38, and B16 murine models. The tumor-infiltrating immune cells in the isotype control samples were compared across tumor models. There was a trend towards more $GITR^+$ cells being present in CT26 tumors (3.2 ± 1% of total live cells) when compared to MC38 tumors (1.8 ± 0.5% of total live cells) and B16 tumors (1.0 ± 0.2% of total live cells), but the difference did not reach statistical significance (one-way ANOVA, $p = 0.1252$) (Figure 2a).

As previously described, tumor Treg depletion correlates with the anti-tumor activity of the GITR antibody DTA-1 in mouse models, and tumor Treg depletion depends on the isotype of the antibody (30,33). The 21B6 antibody had similar characteristics, with mIgG2a mediating tumor Treg depletion compared to isotype control (Supplementary Fig 1a), which was dose-dependent. This effect was not observed with mIgG1 21B6 molecules (Supplementary Fig 1b). Thus, we hypothesized that tumors with a dominant Treg infiltrate would benefit more from GITR antibody treatment. However, the frequency of tumor-infiltrating $CD4^+Foxp3^+CD25^+$ Tregs did not correlate with efficacy of CT26. MC38 tumors contained a higher frequency of Tregs in the immune infiltrate than did CT26 tumors but

Author Manuscript Author Manuscript Author Manuscript Author Manuscript

showed decreased response to anti-GITR therapy (7.6 ± 0.5% versus 3.5 ± 0.7% of $CD45^+$ cells, respectively) (Figure 2b).

CD4 and CD8 T cells are required for successful immunotherapy with most T cell targeting mechanisms. In the models we investigated, the frequency of both effector CD4 ($CD4^+FOXP3^-$) and CD8 T cells correlated with response to GITR antibody: CT26 tumors had the highest frequencies of effector CD4 T cells (5.3 ± 0.9% of $CD45^+$) and CD8 T cells (41.6 ± 5.5% of $CD45^+$) in the immune infiltrate, followed by MC38 tumors (CD4, 3.3 ± 0.5% of $CD45^+$; CD8, 13.5 ± 1.1% of $CD45^+$) and B16 tumors (CD4, 1.9 ± 0.4% of $CD45^+$; CD8, 8.9 ± 2.0% of $CD45^+$) (Figure 2c, d). Furthermore, the frequencies of effector CD4 and CD8 T cells correlated with tumor growth inhibition and survival in these mouse models (Figure 1). The proportion of GITR+ cells within the Treg and effector CD4 T cell populations was similar across the tumor models (Figure 2e, f), but B16 tumors had a significantly higher proportion of $GITR^+$ CD8 T cells than CT26 tumors did (Figure 2g).

Taken together these results showed that in the CT26, MC38, and B16 murine tumor models, the frequency of effector CD8 T cells and CD4 T cells within the immune infiltrate correlates with response to treatment with GITR antibody.

GITR expression within the tumor microenvironment in tumor samples from patients is associated with a high frequency of tumor-infiltrating lymphocytes.

Advanced hepatocellular carcinoma (HCC), non-small cell lung cancer (NSCLC), renal cell carcinoma (RCC), pancreatic carcinoma (PaCa), head and neck carcinoma (H&N), melanoma (Mel), and ovarian carcinoma (OvCa) are lethal diseases that show a range (low to high) of responses to immunotherapies. To determine which of these malignancies should be prioritized for the clinical development of anti-GITR therapies, we evaluated each tumor type for GITR expression using two platforms, IHC and FC. Tumor samples from 213 patients were evaluated by IHC, and tumor samples from 63 patients were evaluated by FC (Table 1). HCC, NSCLC, and RCC were analyzed by both IHC and FC; pancreatic carcinoma and head and neck carcinoma were analyzed only by IHC; and ovarian carcinoma and melanoma were analyzed only by FC (Table 1).

IHC analyses were performed with anti-GITR antibody (Pfizer proprietary, Supplementary Figure 2). To our knowledge, this proprietary anti-GITR antibody is the first anti-GITR antibody validated for IHC for human tumor samples. Immunohistochemical analysis showed that GITR expression on TILs was highest in NSCLC (4.1 ± 1.9%), lower in head and neck carcinoma and RCC (2.40 ± 2.88% and 1.55 ± 0.90%, respectively), and lowest in HCC and pancreatic carcinoma (0.31 ± 0.31% and 0.09 ± 0.09%, respectively) (Figure 3a, 3d and, Supplementary Figure 8e). The frequency of CD8 T cells was significantly higher in NSCLC and RCC (12.32 ± 7.48% and 12.97 ± 10.24%, respectively) than in HCC, pancreatic carcinoma, and head and neck carcinoma (7.35 ± 4.56%, 6.25 ± 5.17%, and 8.31 ± 3.63%, respectively) (Figure 3b, 3d and Supplementary Figure 8d). Similarly, significant differences were observed in CD4 T cells, with higher frequency in NSCLC and RCC (15.52 ± 7.44% and 13.37 ± 7.50%, respectively) and lower frequency in HCC, pancreatic carcinoma, and head and neck carcinoma (7.62 ± 4.69%, 6.82 ± 3.98%, and 7.46 ± 5.83%,

Author Manuscript Author Manuscript Author Manuscript Author Manuscript

respectively) (Figure 3c, 3d and Supplementary Figure 8d). These data demonstrate that GITR expression within the tumor microenvironment varies with tumor type.

We examined the relationship between expression of GITR, CD3, CD4, CD8, and FOXP3 as computed by IHC and FC for 3 tumor types, HCC, NSCLC, and RCC, and observed a good correlation between the two methodologies despite the lower number of samples analyzed by flow cytometry, ($R^2 = 0.78$) (Figure 3e). The coefficient of correlation (R) of each parameter (CD3, CD4, CD8, FOXP3 and GITR) was calculated against the remaining parameters using the values from IHC and FC for each tumor. For IHC, correlation was strong (R>0.65) only for the correlation of CD3/CD4 and CD3/CD8 populations for HCC, RCC, and NSCLC (Supplementary Figure 3a). For FC, correlation was very strong, especially of CD3 with CD4 and CD8 for all tumors (R>=0.76). GITR was also well correlated with CD3, CD4, and CD8 (Supplementary Figure 3b). In summary, these findings show that GITR-expressing CD4 and CD8 T cells exhibit similar trends in expression in NSCLC, RCC, and HCC by both IHC and FC.

GITR is highly expressed on tumor-infiltrating Tregs independent of tumor type.

GITR is highly expressed on activated CD4 and CD8 T cells (15–17) and $FoxP3^+$ Tregs from peripheral blood (18). Since we found an association between GITR expression and T cell infiltration within the tumor microenvironment (Figure 3), here we used FC to quantitate GITR expression within the tumor-infiltrating lymphocyte (TIL) compartment. We found that independent of the tumor type, the percentage of $GITR^+$ cells was highest in the $FoxP3^+$ Treg subpopulation (34.57%, 38.84%, 39.46% and 40.65% of CD4 positive Tregs in HCC, NSCLC, RCC and Mel, respectively), lower in effector CD4 T cells (6.00%, 11.51%, 8.00% and 18.02% of effector CD4 T cells in HCC, NSCLC, RCC and Mel, respectively), and lowest in effector CD8 T cells (1.35%, 6.02%, 3.40% and 6.10% of CD8 T cells in HCC, NSCLC, RCC and Mel, respectively) (Figure 4; results for ovarian carcinoma are shown in Supplementary Figure 4a). The percentage of GITR-expressing cells among Tregs and effector T (Teff) cells ($CD4^+/CD8^+$) for HCC, NSCLC, RCC, melanoma, and ovarian carcinoma is summarized in Supplementary Figure 4b.

Prior preclinical studies have shown that monoclonal antibodies targeting GITR, CTLA-4, and OX40 can induce an Fc-dependent selective depletion of tumoral Tregs that express higher levels of GITR, CTLA-4, and OX40 than do Teff cells in the tumor (30,32–35). Therefore, we sought to determine which T cell subpopulation had higher expression of GITR. We computed the amount of GITR expressed on a per-cell basis (expressed in terms of mean fluorescence intensity [MFI]) within each T cell population. There is a positive relationship between MFI and the density of antibody binding to a cell and therefore between MFI and the number of molecules on a given cell type (36). Consistent with preclinical data and previously published reports, we observed that GITR expression was higher on Tregs than on CD4 Teff or CD8 Teff cells, and this difference was statistically significant across tumor types (Figure 5 and Supplementary Figure 5). This pattern of GITR expression was consistent with that observed in the three mouse tumor models studied (Supplementary Figure 6).

Author Manuscript Author Manuscript Author Manuscript Author Manuscript

DISCUSSION

Taken together, these findings showed that all tumor types analyzed in this study had higher expression of GITR on Tregs than on Teff cells, which is in concordance with preclinical data. This observation suggests that therapeutic antibody development should focus on modulation of tumor-infiltrating Tregs. IHC and FC data suggest that NSCLC, RCC, and melanoma should be given high priority for the development of anti-GITR therapies as all three types of tumors exhibit high frequency of GITR-expressing TILs and/or high Treg GITR expression on a per-cell basis.

While long-lasting tumor regression is seen with some immune-targeting antibody-based therapies, a significant proportion of patients still do not respond. The field is rapidly evolving to a deeper understanding of the immunological signatures that may predict responders to immune-targeting therapies. Higher expression of the immunotherapy target in the tumor tends to be positively correlated with response to treatment in some tumor types. For example, metastatic bladder cancer with greater PD-L1 expression in the tumor is more likely to respond to the anti-PD-L1 antibody atezolizumab (8). Similarly, metastatic melanoma with higher numbers of PD-1^+ cells and CD8 T cells within the tumor stroma and tumor bed may be more likely to respond to pembrolizumab (14). Daud and colleagues showed that PD-1 expression, and specifically, increased tumor infiltration of PD-1^+CTLA-4^+ effector CD8 T cells, correlates with response of metastatic melanoma to pembrolizumab or nivolumab (37). The presence of lymphocyte infiltrates and cytotoxic immune cell signatures in tumors is associated with improved survival in most cancer types, including NSCLC, colorectal carcinoma, and melanoma (38,39). These findings have led to a model in which tumors are classified as “hot” or “cold” to reflect grading of the immune infiltrate (40–42). It is therefore essential to evaluate the baseline tumor expression of the target and the extent of CD8 T cell infiltration in the tumor to establish correlations with responses in clinical trials of cancer immunotherapies.

GITR expression in human tumors has not been well characterized, in part because of the lack of a validated IHC antibody. To our knowledge, this is the first report of GITR expression in patient derived tumor tissue analyzed by IHC. During the work described herein, we successfully established evaluation of GITR expression with a proprietary antibody by IHC. In addition, in our concomitant analysis using FC with commercial antibodies, we established the correlatives of these orthogonal platforms. Tumor biopsies are amenable to IHC analysis, which keeps the architectural information, but allows for fewer parameters to be analyzed. FC analysis allows more parameters to be analyzed simultaneously but does not provide architectural context. In the study reported here, HCC, NSCLC, and RCC samples were evaluated by both of these platforms head to head. The frequencies of CD3, CD4, CD8, and GITR$^+$ cells were similar with FC and IHC even though FC uses fluorochromes in a single cell suspension and IHC uses an enzymatic reaction on a slide. The slight difference between the results from IHC and FC can be partly explained by differences in the number of samples available for analysis using each method: more samples were available for IHC analysis (range 23-60) than for FC analysis (range 10-16), which meant that in some cases differences across tumors types were statistically significant for IHC but only suggestive of a trend for FC analysis. Markers expressed at a high

Author Manuscript Author Manuscript Author Manuscript Author Manuscript

frequency (e.g., CD3) or low frequency (e.g., GITR) on IHC showed similar expression pattern in FC, with a very strong correlation between the median values of each marker on IHC and FC (R^2= 0.78).

Even if the number of samples available for FC was lower than the ones available for IHC, we found a strong correlation for these two methods. We used IHC to determine which solid tumors expressed more immune markers (CD3, CD4, CD8, and GITR) and used FC to gain complementary information on the subpopulations expressing GITR (CD4 Tregs/Teff cells or CD8 T cells) and the intensity of expression of GITR on these cell subpopulations (using MFI as a readout). On the basis of our findings, we can conclude that head and neck carcinoma had a high frequency of $GITR^+$ cells but low frequency of CD4 and CD8 T cell infiltration, whereas NSCLC, RCC, and melanoma had a high frequency of GITR+ cells together with a high frequency of CD4 and CD8 T cell infiltration, as shown by IHC (Figure 3 and Supplementary Figures 4b and 5b).

In mouse models, two non-exclusive mechanisms of anti-tumor effect from GITR antibody treatment have been proposed. First, it has been reported that GITR agonistic antibody can act by directly down-regulating Treg expression of FoxP3 and abrogating the suppressive function of Tregs (23), and by augmenting the resistance of antigen-specific CD8 T cells to Treg suppression (43,44). Second, more recent studies have implicated tumor-associated myeloid cells mediating antibody-dependent phagocytosis of intratumoral Tregs by activating Fcγ Rs (30,33,45). Given the reported mechanism of action of GITR antibodies acting primarily on tumor-infiltrating Tregs in tumor-bearing mice, it is essential to compare GITR expression patterns in solid tumors of humans and mouse to assess the suitability of mouse tumor models for studies of the therapeutic efficacy of GITR antibody and underlying mechanisms. Indeed, DTA-1 induced selective reduction of circulating Tregs in a mouse model (45). In the MB49 tumor model of chemically induced murine bladder carcinoma and the CT26 colon adenocarcinoma tumor model, depletion of Tregs took place preferentially in tumors and not in tumor-draining lymph nodes, a finding attributed to higher levels of GITR expression on tumor-infiltrating Tregs than on Tregs in tumor-draining lymph nodes (33,45). This strongly suggests that the efficiency of depletion might be correlated with the level of GITR expression and the proportion of FcγR-expressing cells in the tumor microenvironment. It is well established that efficient antibody-mediated depletion of cells correlates with receptor density (46).

We found, in agreement with what has previously been published (18), that GITR was expressed at higher frequencies in all tumoral $CD4^+$ $Foxp3^+$ Tregs analyzed than in effector CD4 T cells or CD8 T cells, regardless of the level of infiltration or the tumor type (Figure 4 and supplementary Figure 4). Thus, HCC, which showed much less infiltration than other tumor types as determined by IHC (Figure 3b and c), also showed a high frequency of CD4 Tregs expressing GITR (Figure 4a). Moreover, the tumors with a high frequency of $GITR^+$ cells together with high frequencies of CD4 and CD8 T cells by IHC (NSCLC, RCC, and melanoma) also showed the highest frequency of GITR-expressing Tregs (about 40%), significantly higher than the frequency of $GITR^+$ Teff cells and CD8 T cells ($P \leq 0.0001$) (Supplementary Figure 4b). RCC, melanoma, and NSCLC, in addition to having high frequencies of $GITR^+$ Tregs, had high numbers of GITR molecules per Treg cell

Author Manuscript Author Manuscript Author Manuscript Author Manuscript

(Supplementary Figure 5b). In contrast, HCC, which had the similar frequency of GITR$^+$ Tregs as RCC, melanoma, and NSCLC (about 40%), had fewer GITR molecules per Treg cell (Figures 4a and 5a). Differences in the levels of GITR expression could be attributed to differences in tumor stage (primary or metastatic), previous therapy, or activation state of the Treg, interactions with cognate antigen or the microenvironment. NSCLC and melanoma have been reported to have a higher mutational load than HCC (47). Thus, NSCLC and melanoma may harbor a higher proportion of neoantigens for presentation to CD4 Tregs by local antigen-presenting cells. In addition, the T cell receptors in Tregs are enriched for reactivity to self-antigen (48) and thus are potentially biased for antigen recognition in tumors. Activation of T cell receptors in Treg may be driving enhanced GITR expression by Tregs infiltrating solid tumors (49).

As stated before, one of the mechanisms that may explain the anti-tumor effect of the agonistic anti-GITR DTA-1 is preferential depletion of Tregs due to the constitutively high expression of GITR in these cells. This would indicate that the human tumors better suited for treatment with anti-GITR antibody to elicit this potential Treg depletion could be NSCLC, RCC, and melanoma (Supplementary Figures 4b and 5b). We are nevertheless aware that murine models may not accurately reflect what the mechanism of anti-tumor effect will be in humans; differences in 1) expression patterns and relative levels of proteins, 2) FcγR biology, 3) tumor lifespans alongwith heterogeneity of molecular phenotypes and stroma likely all contribute.

In conclusion, results of our comparison of FC and IHC indicate that single-stain IHC is comparable to FC for determining the abundance of GITR-expressing cells in formalin-fixed, paraffin-embedded tumor tissue. Our mouse data suggest that FcγR-binding GITR antibodies have the greatest therapeutic benefit in tumors that have a higher abundance of tumor infiltrating CD8 T cells. Thus, considering positive correlations of benefit and CD8 T cell and GITR levels, from all the tumor types surveyed by IHC and FC in our study (HCC, NSCLC, RCC, pancreatic carcinoma, head and neck carcinoma, ovarian carcinoma and melanoma), we would suggest prioritizing NSCLC, RCC and melanoma for treatment with a FcγR-binding GITR antibody.

Supplementary Material

Refer to Web version on PubMed Central for supplementary material.

Acknowledgments

Financial support: Supported by Pfizer Inc.

REFERENCES

1. Hodi FS, O'Day SJ, McDermott DF, Weber RW, Sosman JA, Haanen JB, et al. Improved survival with ipilimumab in patients with metastatic melanoma. The New England journal of medicine 2010;363(8):711–23 doi 10.1056/NEJMoa1003466. [PubMed: 20525992]
2. Robert C, Schachter J, Long GV, Arance A, Grob JJ, Mortier L, et al. Pembrolizumab versus Ipilimumab in Advanced Melanoma. The New England journal of medicine 2015;372(26):2521–32 doi 10.1056/NEJMoa1503093. [PubMed: 25891173]

Author Manuscript Author Manuscript Author Manuscript Author Manuscript

3. Robert C, Thomas L, Bondarenko I, O'Day S, Weber J, Garbe C, et al. Ipilimumab plus dacarbazine for previously untreated metastatic melanoma. The New England journal of medicine 2011;364(26): 2517–26 doi 10.1056/NEJMoa1104621. [PubMed: 21639810]

4. Weber JS, D'Angelo SP, Minor D, Hodi FS, Gutzmer R, Neyns B, et al. Nivolumab versus chemotherapy in patients with advanced melanoma who progressed after anti-CTLA-4 treatment (CheckMate 037): a randomised, controlled, open-label, phase 3 trial. Lancet Oncol 2015;16(4): 375–84 doi 10.1016/S1470-2045(15)70076-8. [PubMed: 25795410]

5. Motzer RJ, Escudier B, McDermott DF, George S, Hammers HJ, Srinivas S, et al. Nivolumab versus Everolimus in Advanced Renal-Cell Carcinoma. The New England journal of medicine 2015;373(19):1803–13 doi 10.1056/NEJMoa1510665. [PubMed: 26406148]

6. Borghaei H, Paz-Ares L, Horn L, Spigel DR, Steins M, Ready NE, et al. Nivolumab versus Docetaxel in Advanced Nonsquamous Non-Small-Cell Lung Cancer. The New England journal of medicine 2015;373(17):1627–39 doi 10.1056/NEJMoa1507643. [PubMed: 26412456]

7. Brahmer J, Reckamp KL, Baas P, Crino L, Eberhardt WE, Poddubskaya E, et al. Nivolumab versus Docetaxel in Advanced Squamous-Cell Non-Small-Cell Lung Cancer. The New England journal of medicine 2015;373(2):123–35 doi 10.1056/NEJMoa1504627. [PubMed: 26028407]

8. Powles T, Eder JP, Fine GD, Braiteh FS, Loriot Y, Cruz C, et al. MPDL3280A (anti-PD-L1) treatment leads to clinical activity in metastatic bladder cancer. Nature 2014;515(7528):558–62 doi 10.1038/nature13904. [PubMed: 25428503]

9. Ansell SM, Lesokhin AM, Borrello I, Halwani A, Scott EC, Gutierrez M, et al. PD-1 blockade with nivolumab in relapsed or refractory Hodgkin's lymphoma. The New England journal of medicine 2015;372(4):311–9 doi 10.1056/NEJMoa1411087. [PubMed: 25482239]

10. Larkin J, Chiarion-Sileni V, Gonzalez R, Grob JJ, Cowey CL, Lao CD, et al. Combined Nivolumab and Ipilimumab or Monotherapy in Untreated Melanoma. The New England journal of medicine 2015;373(1):23–34 doi 10.1056/NEJMoa1504030. [PubMed: 26027431]

11. Hugo W, Zaretsky JM, Sun L, Song C, Moreno BH, Hu-Lieskovan S, et al. Genomic and Transcriptomic Features of Response to Anti-PD-1 Therapy in Metastatic Melanoma. Cell 2016;165(1):35–44 doi 10.1016/j.cell.2016.02.065. [PubMed: 26997480]

12. Rizvi NA, Hellmann MD, Snyder A, Kvistborg P, Makarov V, Havel JJ, et al. Cancer immunology. Mutational landscape determines sensitivity to PD-1 blockade in non-small cell lung cancer. Science 2015;348(6230):124–8 doi 10.1126/science.aaa1348. [PubMed: 25765070]

13. Topalian SL, Hodi FS, Brahmer JR, Gettinger SN, Smith DC, McDermott DF, et al. Safety, activity, and immune correlates of anti-PD-1 antibody in cancer. The New England journal of medicine 2012;366(26):2443–54 doi 10.1056/NEJMoa1200690. [PubMed: 22658127]

14. Tumeh PC, Harview CL, Yearley JH, Shintaku IP, Taylor EJ, Robert L, et al. PD-1 blockade induces responses by inhibiting adaptive immune resistance. Nature 2014;515(7528):568–71 doi 10.1038/nature13954. [PubMed: 25428505]

15. Nocentini G, Giunchi L, Ronchetti S, Krausz LT, Bartoli A, Moraca R, et al. A new member of the tumor necrosis factor/nerve growth factor receptor family inhibits T cell receptor-induced apoptosis. Proceedings of the National Academy of Sciences of the United States of America 1997;94(12):6216–21. [PubMed: 9177197]

16. Nocentini G, Ronchetti S, Petrillo MG, Riccardi C. Pharmacological modulation of GITRL/GITR system: therapeutic perspectives. British journal of pharmacology 2012;165(7):2089–99 doi 10.1111/j.1476-5381.2011.01753.x. [PubMed: 22029729]

17. Schaer DA, Murphy JT, Wolchok JD. Modulation of GITR for cancer immunotherapy. Current opinion in immunology 2012;24(2):217–24 doi 10.1016/j.coi.2011.12.011. [PubMed: 22245556]

18. Shimizu J, Yamazaki S, Takahashi T, Ishida Y, Sakaguchi S. Stimulation of CD25(+)CD4(+) regulatory T cells through GITR breaks immunological self-tolerance. Nature immunology 2002;3(2):135–42 doi 10.1038/ni759. [PubMed: 11812990]

19. Kohrt HE, Houot R, Goldstein MJ, Weiskopf K, Alizadeh AA, Brody J, et al. CD137 stimulation enhances the antilymphoma activity of anti-CD20 antibodies. Blood 2011;117(8):2423–32 doi 10.1182/blood-2010-08-301945. [PubMed: 21193697]

20. Hanabuchi S, Watanabe N, Wang YH, Wang YH, Ito T, Shaw J, et al. Human plasmacytoid predendritic cells activate NK cells through glucocorticoid-induced tumor necrosis factor receptor-

Author Manuscript Author Manuscript Author Manuscript Author Manuscript

ligand (GITRL). Blood 2006;107(9):3617–23 doi 10.1182/blood-2005-08-3419. [PubMed: 16397134]

21. Ronchetti S, Zollo O, Bruscoli S, Agostini M, Bianchini R, Nocentini G, et al. GITR, a member of the TNF receptor superfamily, is costimulatory to mouse T lymphocyte subpopulations. European journal of immunology 2004;34(3):613–22 doi 10.1002/eji.200324804. [PubMed: 14991590]
22. Snell LM, Lin GH, McPherson AJ, Moraes TJ, Watts TH. T-cell intrinsic effects of GITR and 4-1BB during viral infection and cancer immunotherapy. Immunological reviews 2011;244(1): 197–217 doi 10.1111/j.1600-065X.2011.01063.x. [PubMed: 22017440]
23. Cohen AD, Schaer DA, Liu C, Li Y, Hirschhorn-Cymmerman D, Kim SC, et al. Agonist anti-GITR monoclonal antibody induces melanoma tumor immunity in mice by altering regulatory T cell stability and intra-tumor accumulation. PloS one 2010;5(5):e10436 doi 10.1371/journal.pone. 0010436. [PubMed: 20454651]
24. Ko K, Yamazaki S, Nakamura K, Nishioka T, Hirota K, Yamaguchi T, et al. Treatment of advanced tumors with agonistic anti-GITR mAb and its effects on tumor-infiltrating Foxp3+CD25+CD4+ regulatory T cells. The Journal of experimental medicine 2005;202(7):885–91 doi 10.1084/jem. 20050940. [PubMed: 16186187]
25. Zhou P, L'Italien L, Hodges D, Schebye XM. Pivotal roles of CD4+ effector T cells in mediating agonistic anti-GITR mAb-induced-immune activation and tumor immunity in CT26 tumors. Journal of immunology 2007;179(11):7365–75.
26. Mitsui J, Nishikawa H, Muraoka D, Wang L, Noguchi T, Sato E, et al. Two distinct mechanisms of augmented antitumor activity by modulation of immunostimulatory/inhibitory signals. Clinical cancer research : an official journal of the American Association for Cancer Research 2010;16(10):2781–91 doi 10.1158/1078-0432.CCR-09-3243.
27. Lu L, Xu X, Zhang B, Zhang R, Ji H, Wang X. Combined PD-1 blockade and GITR triggering induce a potent antitumor immunity in murine cancer models and synergizes with chemotherapeutic drugs. Journal of translational medicine 2014;12:36 doi 10.1186/1479-5876-12-36. [PubMed: 24502656]
28. Henry B Koon DRS, Taha Merghoub, David A. Schaer, Cynthia A. Sirard, Jedd D. Wolchok. First-in-human phase 1 single-dose study of TRX-518, an anti-human glucocorticoid-induced tumor necrosis factor receptor (GITR) monoclonal antibody in adults with advanced solid tumors. 2016 2016; Chicago, IL. J Clin Oncol 34, 2016 (suppl; abstr 3017).
29. Zappasodi RL Yanyun & Abu-Akeel Mohsen & Qi Jingjing & Wong Philip & Sirard Cynthia & Postow Michael & Schaer David & Newman Walter & Koon Henry & Velcheti Vamsidhar & K. Callahan Margaret & D. Wolchok Jedd & Merghoub Taha. Abstract CT018: Intratumor and peripheral Treg modulation as a pharmacodynamic biomarker of the GITR agonist antibody TRX-518 in the first in-human trial. Cancer research 2017;77(CT018-CT018):1538–7445.
30. Mahne AE, Mauze S, Joyce-Shaikh B, Xia J, Bowman EP, Beebe AM, et al. Dual Roles for Regulatory T-cell Depletion and Costimulatory Signaling in Agonistic GITR Targeting for Tumor Immunotherapy. Cancer research 2017;77(5):1108–18 doi 10.1158/0008-5472.CAN-16-0797. [PubMed: 28122327]
31. DiLillo DJ, Ravetch JV. Fc-Receptor Interactions Regulate Both Cytotoxic and Immunomodulatory Therapeutic Antibody Effector Functions. Cancer Immunol Res 2015;3(7):704–13 doi 10.1158/2326-6066.CIR-15-0120. [PubMed: 26138698]
32. Bulliard Y, Jolicoeur R, Zhang J, Dranoff G, Wilson NS, Brogdon JL. OX40 engagement depletes intratumoral Tregs via activating FcgammaRs, leading to antitumor efficacy. Immunol Cell Biol 2014;92(6):475–80 doi 10.1038/icb.2014.26. [PubMed: 24732076]
33. Bulliard Y, Jolicoeur R, Windman M, Rue SM, Ettenberg S, Knee DA, et al. Activating Fc gamma receptors contribute to the antitumor activities of immunoregulatory receptor-targeting antibodies. The Journal of experimental medicine 2013;210(9):1685–93 doi 10.1084/jem.20130573. [PubMed: 23897982]
34. Selby MJ, Engelhardt JJ, Quigley M, Henning KA, Chen T, Srinivasan M, et al. Anti-CTLA-4 antibodies of IgG2a isotype enhance antitumor activity through reduction of intratumoral regulatory T cells. Cancer Immunol Res 2013;1(1):32–42 doi 10.1158/2326-6066.CIR-13-0013. [PubMed: 24777248]

Author Manuscript Author Manuscript Author Manuscript Author Manuscript

35. Simpson TR, Li F, Montalvo-Ortiz W, Sepulveda MA, Bergerhoff K, Arce F, et al. Fc-dependent depletion of tumor-infiltrating regulatory T cells co-defines the efficacy of anti-CTLA-4 therapy against melanoma. The Journal of experimental medicine 2013;210(9):1695–710 doi 10.1084/jem.20130579. [PubMed: 23897981]
36. Moskalensky AE, Chernyshev AV, Yurkin MA, Nekrasov VM, Polshchitsin AA, Parks DR, et al. Dynamic quantification of antigen molecules with flow cytometry. J Immunol Methods 2015;427:139–47. [PubMed: 27030828]
37. Daud AI, Loo K, Pauli ML, Sanchez-Rodriguez R, Sandoval PM, Taravati K, et al. Tumor immune profiling predicts response to anti-PD-1 therapy in human melanoma. J Clin Invest 2016;126(9):3447–52 doi 10.1172/JCI87324. [PubMed: 27525433]
38. Gibney GT, Weiner LM, Atkins MB. Predictive biomarkers for checkpoint inhibitor-based immunotherapy. Lancet Oncol 2016;17(12):e542–e51 doi 10.1016/S1470-2045(16)30406-5. [PubMed: 27924752]
39. Hegde PS, Karanikas V, Evers S. The Where, the When, and the How of Immune Monitoring for Cancer Immunotherapies in the Era of Checkpoint Inhibition. Clinical cancer research : an official journal of the American Association for Cancer Research 2016;22(8):1865–74 doi 10.1158/1078-0432.CCR-15-1507.
40. Gajewski TF. The Next Hurdle in Cancer Immunotherapy: Overcoming the Non-T-Cell-Inflamed Tumor Microenvironment. Semin Oncol 2015;42(4):663–71 doi 10.1053/j.seminoncol.2015.05.011. [PubMed: 26320069]
41. Palucka AK, Coussens LM. The Basis of Oncoimmunology. Cell 2016;164(6):1233–47 doi 10.1016/j.cell.2016.01.049. [PubMed: 26967289]
42. Spranger S Mechanisms of tumor escape in the context of the T-cell-inflamed and the non-T-cell-inflamed tumor microenvironment. Int Immunol 2016;28(8):383–91 doi 10.1093/intimm/dxw014. [PubMed: 26989092]
43. Nishikawa H, Kato T, Hirayama M, Orito Y, Sato E, Harada N, et al. Regulatory T cell-resistant CD8+ T cells induced by glucocorticoid-induced tumor necrosis factor receptor signaling. Cancer research 2008;68(14):5948–54 doi 10.1158/0008-5472.CAN-07-5839. [PubMed: 18632650]
44. Stephens GL, McHugh RS, Whitters MJ, Young DA, Luxenberg D, Carreno BM, et al. Engagement of glucocorticoid-induced TNFR family-related receptor on effector T cells by its ligand mediates resistance to suppression by CD4+CD25+ T cells. Journal of immunology 2004;173(8):5008–20.
45. Coe D, Begom S, Addey C, White M, Dyson J, Chai JG. Depletion of regulatory T cells by anti-GITR mAb as a novel mechanism for cancer immunotherapy. Cancer immunology, immunotherapy : CII 2010;59(9):1367–77 doi 10.1007/s00262-010-0866-5. [PubMed: 20480365]
46. Niwa R, Sakurada M, Kobayashi Y, Uehara A, Matsushima K, Ueda R, et al. Enhanced natural killer cell binding and activation by low-fucose IgG1 antibody results in potent antibody-dependent cellular cytotoxicity induction at lower antigen density. Clinical cancer research : an official journal of the American Association for Cancer Research 2005;11(6):2327–36 doi 10.1158/1078-0432.CCR-04-2263.
47. Alexandrov LB, Nik-Zainal S, Wedge DC, Aparicio SA, Behjati S, Biankin AV, et al. Signatures of mutational processes in human cancer. Nature 2013;500(7463):415–21 doi 10.1038/nature12477. [PubMed: 23945592]
48. Lee HM, Bautista JL, Hsieh CS. Thymic and peripheral differentiation of regulatory T cells. Adv Immunol 2011;112:25–71 doi 10.1016/B978-0-12-387827-4.00002-4. [PubMed: 22118406]
49. Ronchetti S, Ricci E, Petrillo MG, Cari L, Migliorati G, Nocentini G, et al. Glucocorticoid-induced tumour necrosis factor receptor-related protein: a key marker of functional regulatory T cells. J Immunol Res 2015;2015:171520 doi 10.1155/2015/171520. [PubMed: 25961057]

Author Manuscript Author Manuscript Author Manuscript Author Manuscript

Translational relevance:

GITR is a member of the TNF receptor superfamily expressed by T cells and other immune cells. GITR agonistic antibodies show tumor growth inhibition and extended survival and depletion of tumor-infiltrating Tregs has been implicated as the primary mechanism of action. Four GITR antibodies are currently being evaluated in clinical trials in patients with solid tumor. We sought to characterize the level and pattern of GITR expression in human tumors, which may give insight into which tumors are more likely to respond to anti-GITR treatment. Seven human solid malignancies were characterized either by immunohistochemistry with a newly validated antibody or by flow cytometry. Out of the seven, three malignancies (HCC, RCC and NSCLC) were evaluated by both techniques. Clinical samples were evaluated for GITR expression on Tregs on a per-cell basis. The results suggest that non-small cell lung cancer, renal cell carcinoma, and melanoma should be given high priority for the development of anti-GITR therapies.

Author Manuscript Author Manuscript Author Manuscript Author Manuscript

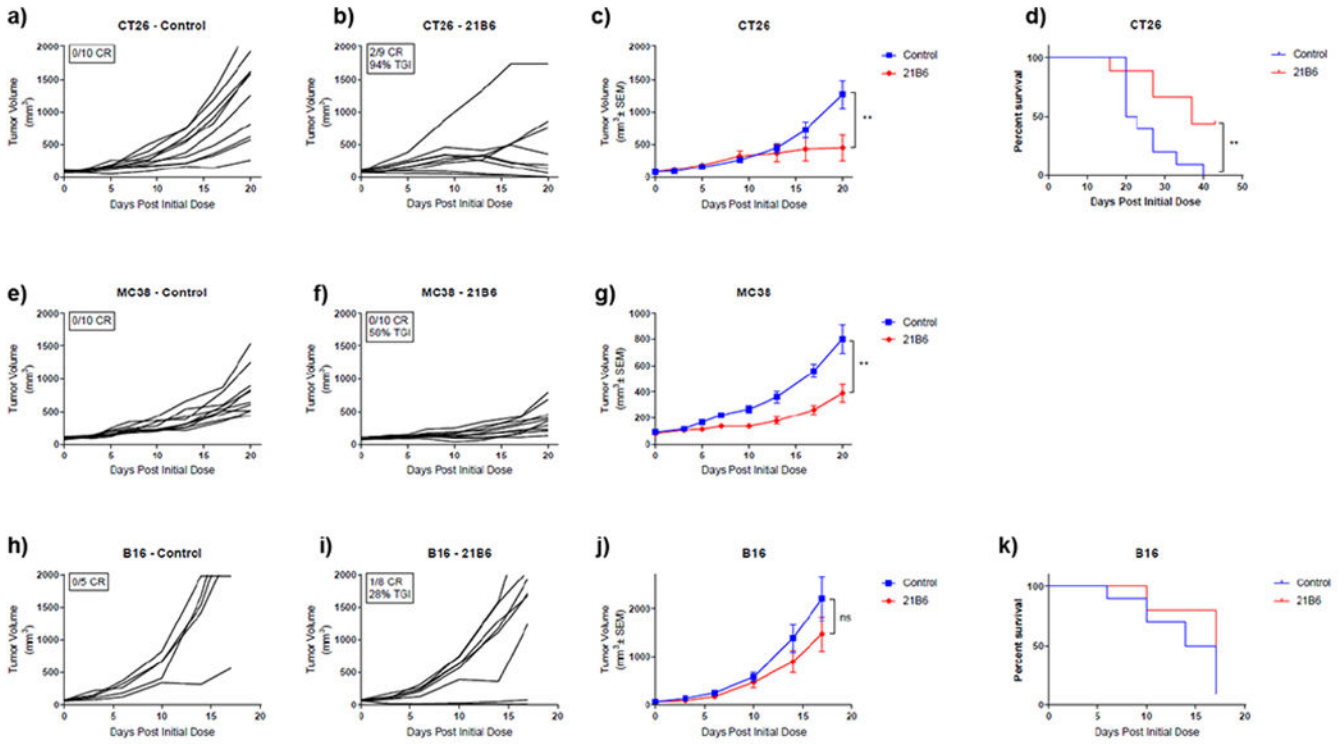

Figure 1. Effect of anti-GITR antibody treatment on three different mouse tumor models.

Three different mouse tumor models, CT26 colon carcinoma (a-d), MC38 colon carcinoma (e-g), and B16 melanoma (h-k), were developed by subcutaneous inoculation of tumor cells. Mice were treated with three doses of anti-GITR antibody 21B6 delivered intraperitoneally. CT26 tumor growth in 21B6-treated mice was inhibited by 94.17% (b) compared to the tumor growth in isotype-treated mice (a). Tumor growth inhibition (c) and survival (d) were significantly greater in 21B6-treated mice than in isotype-control-treated mice. 21B6 was less effective against MC38 tumors: tumor growth in 21B6-treated mice was inhibited by 57.85% (f) compared to the tumor growth in control mice (e), and this inhibition was significant (g). Survival could not be calculated in the MC38 model because of tumor ulceration. 21B6 had the least therapeutic benefit for B16 tumors, in which 21B6 resulted in 27.85% tumor growth inhibition (i, j) compared to the tumor growth in control mice (h), and no survival improvement (k). Data are representative of 2–4 experiments per tumor model. CR, complete response; TGI, tumor growth inhibition. **, $p \leq 0.01$.

Author Manuscript Author Manuscript Author Manuscript Author Manuscript

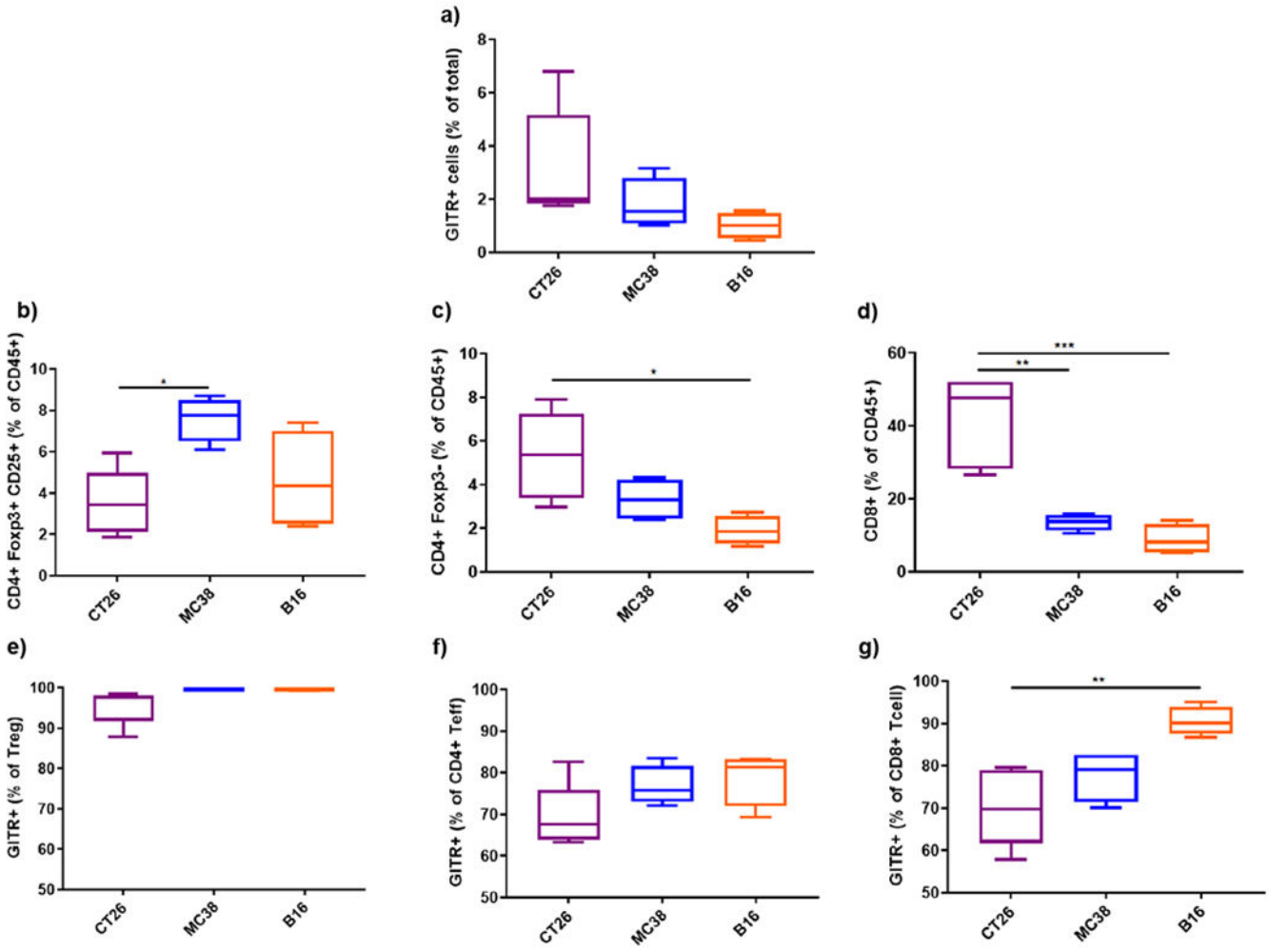

Figure 2. The frequency of effector T cells (CD8 and CD4) in three different mouse tumor models correlates with response to anti-GITR antibody.

TILs were profiled by FC 2 days after the third and final antibody treatment. Shown are the percentages of TILs expressing GITR (a); the frequencies of TILs that were CD4 Tregs (b), CD4 Teff cells (c), and CD8 T cells (d); and the frequencies of $GITR^+$ cells within the CD4 Treg (e), CD4 Teff cell (f), and CD8 T cell (g) TIL fractions. *, $p \leq 0.05$; **, $p \leq 0.01$; ***, $p \leq 0.001$ by 1-way ANOVA followed by Tukey's multiple comparison test.

Author Manuscript Author Manuscript Author Manuscript Author Manuscript

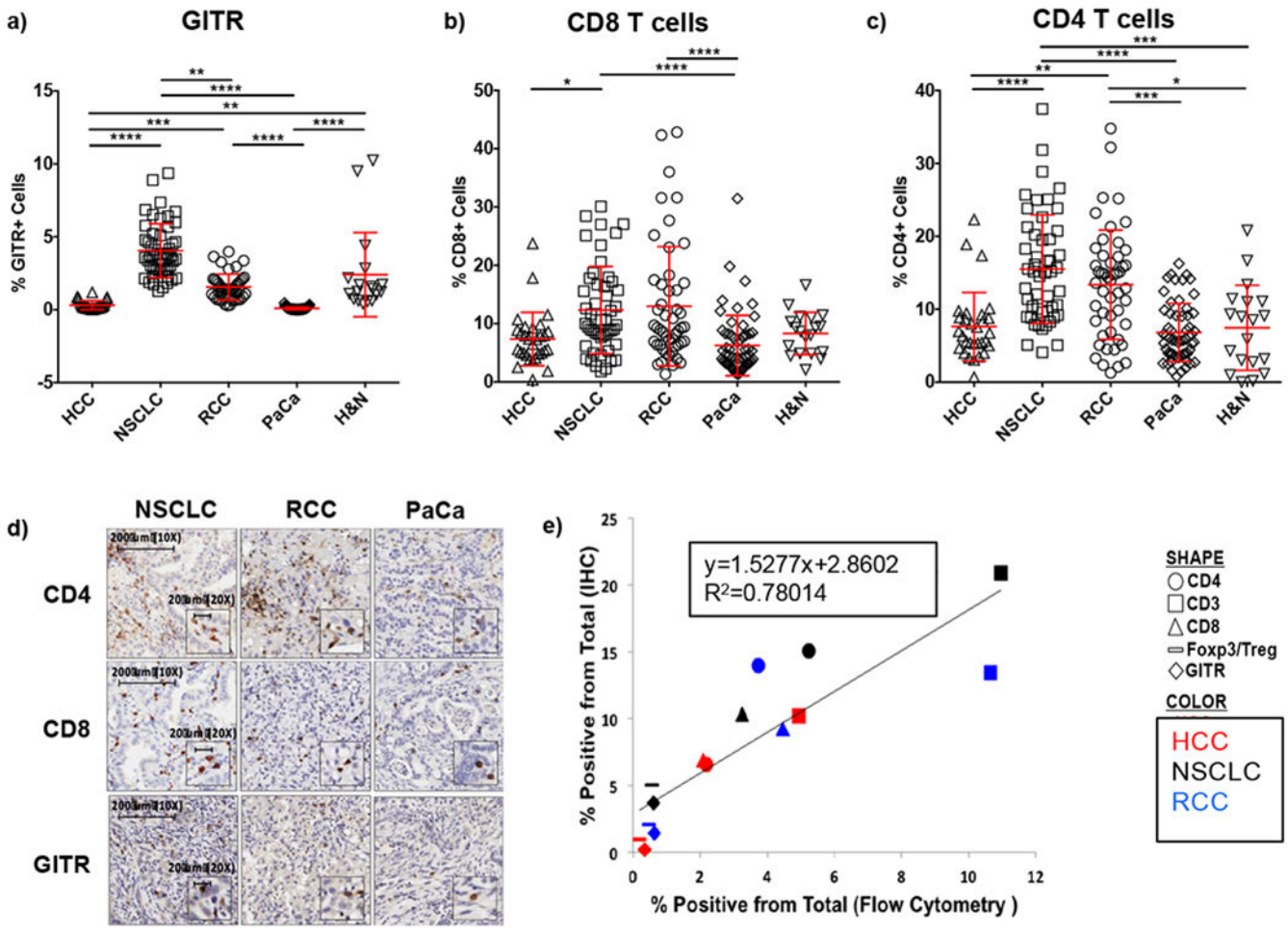

Figure 3. GITR expression within the tumor microenvironment is associated with a high frequency of TILs.

(a-c) IHC analyses of (a) GITR expression, (b) CD8 expression, and (c) CD4 expression in HCC, NSCLC, RCC, pancreatic carcinoma (PaCa), and head and neck carcinoma (H&N). (c) Representative single stain IHC images showing CD4; CD8; GITR expression in NSCLC, RCC and PaCa. (e) Regression analysis showing comparison of findings of IHC and FC from the three tumor types analyzed by both methods using regression showing expression of CD4, CD3, CD8, Treg/Foxp3, and GITR. The two methods showed strong positive correlation for HCC, NSCLC, and RCC. *, $p \leq 0.05$; **, $p \leq 0.01$; ***, $p \leq 0.001$; ****, $p \leq 0.0001$. Numbers of tumor samples analyzed are shown in Table 1.

Author Manuscript Author Manuscript Author Manuscript Author Manuscript

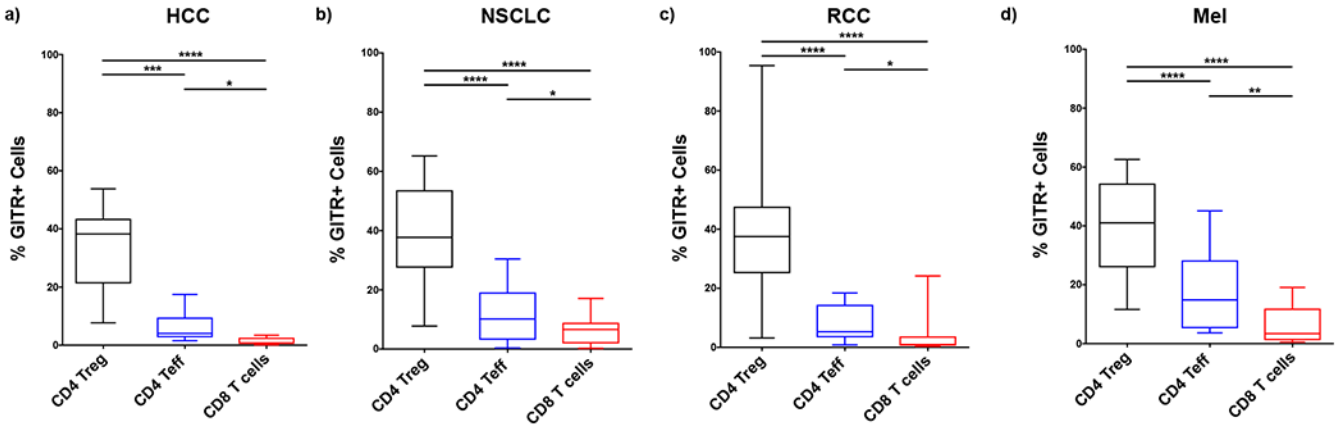

Figure 4. The frequency of expression of GITR is higher in Tregs than in effector T cells (CD4 and CD8).

Using FC, the frequencies of $GITR^+$ cells as a fraction of CD4 Tregs, CD4 Teff cells, and CD8 T cells were calculated for HCC (a), NSCLC (b), RCC (c) and Melanoma (d). *, $p \leq 0.05$; **, $p \leq 0.01$; ***, $p \leq 0.001$; ****, $p \leq 0.0001$. Numbers of tumor samples analyzed are shown in Table 1.

Author Manuscript Author Manuscript Author Manuscript Author Manuscript

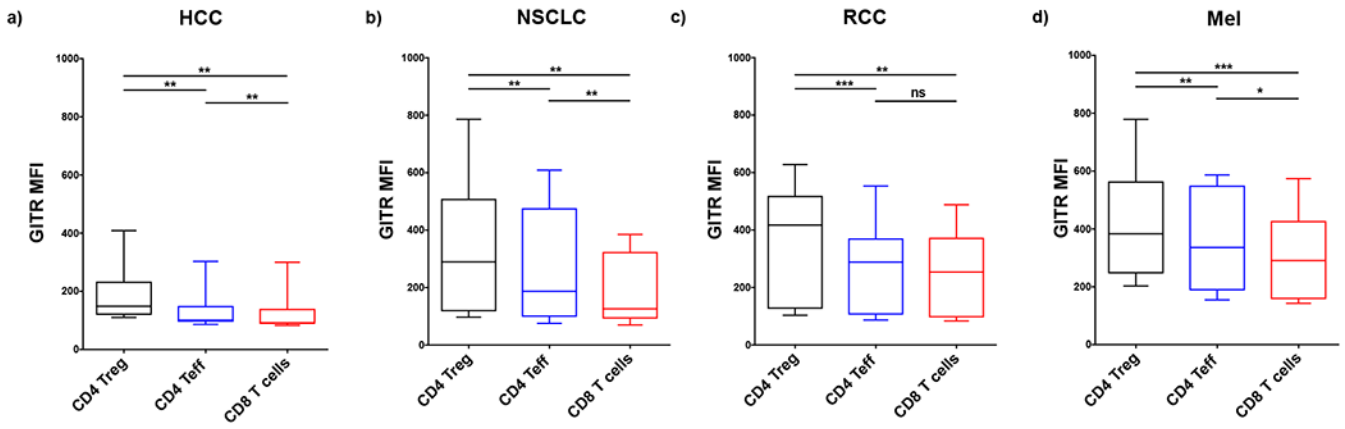

Figure 5. The amount of GITR on a per-cell basis is higher in Tregs than in effector T cells (CD4 and CD8).

Using FC, the MFI of $CD4^+GITR^+$ Tregs, $CD4^+GITR^+$ Teff cells, and $CD8^+GITR^+$ T cells was measured in HCC (a), NSCLC (b) RCC (c) and Mel (d). * indicates, $p \leq 0.05$; **, $p \leq 0.01$; ***, $p \leq 0.001$; ****, $p \leq 0.0001$. Numbers of tumor samples analyzed are shown in Table 1.

Author Manuscript

Author Manuscript

Author Manuscript

Author Manuscript

Table 1.

Number of samples per tumor type used for Flow Cytometry analysis and Immunohistochemistry.

Number of samples per assay	Tumor Type							Totals
	HCC	NSCLC	RCC	OvCa	Mel	PaCa	H&N	
Immunohistochemistry	30	50	50	0	0	60	23	213
Flow Cytometry	10	16	14	11	12	0	0	63

OvCa, ovarian carcinoma; Mel, melanoma; PaCa, pancreatic carcinoma; H&N, head and neck carcinoma